

Fig. 3.39 A scan of the revolution time, from 0.02 to 1 MeV, and its dependence on the field index k . The right vertical axis only concerns the case $k = 0$ where the change in revolution time is weak and only due to the mass increase (in $T_{\text{rev}} = 2\pi\gamma m_0/qB$). The right graph shows, up to 5 MeV, the relatively important contribution of the focusing index, even a weak $k=-0.03$, compared to the effect of the mass increase ($k=0$ curve). Markers are from raytracing, solid lines are from theory

2587 3.8 Ion Trajectories

2588 A zgoubi data file is set up for computation of particle trajectories, taking a
2589 field value on reference radius of $B_0(R_0) = 0.5$ T, and reference energy 200 keV
2590 (proton). These hypotheses determine the reference radius value. DIPOLE [16,
2591 *lookup* INDEX] is used (Tab. 3.21), for its greater flexibility in changing magnet
2592 parameters, field and radial field index amongst other, compared to using TOSCA
2593 and a field map.

2594 (a) Transverse motion.

2595 It first has to be checked that there is consistency between initial orbital radius
2596 Y_0 in OBJET at 200 keV proton energy and the value of the reference radius R_0 in
2597 DIPOLE (Eq. 3.35). Its theoretical value is $R_0 = BORO/5[kG] = 12.924889$ cm, a
2598 closed orbit finding using FIT can be performed, or it can be referred to the solutions
2599 of earlier exercises, to check agreement with raytracing outcomes.

2600 (b) Wave numbers at 1 and 5 MeV.

2601 These considerations result in the input data file given in Tab. 3.22, to compute
2602 multiturn trajectories. ; note that $R_0 = 12.924889$ cm therein, whereas a value of
2603 $R_0 = 50$ cm may be taken instead in other exercises. Field index derivatives k' , k'' , ...
2604 are taken null in the present exercise.

2605 Three particles with paraxial radial and axial motions are raytraced over a few
2606 turns. Their starting radius is the closed orbit radius for the respective energies, while
2607 a 0.1 mrad take-off angle is imparted to each particle both vertically and horizontally.

The value of the focusing index k_E at an energy E can be expressed in terms of DIPOLE data which are, the index value k at R_0 (Eq. 3.11), reference radius R_0 , and field $B_0 = B_Z(R_0)$, namely,

$$k_E = \frac{R_E}{B_E} \frac{\partial B}{\partial R} = \frac{R_0 + \Delta R}{B_0 + \Delta B} \frac{\partial B}{\partial R} \approx k \frac{1 + \Delta R/R_0}{1 + k\Delta R/R_0} \approx k \left[1 + (1 - k) \frac{\Delta R}{R_0} \right]$$

Table 3.21 Input data file 60DegSectorR200.inc: it defines DIPOLE as a sequence segment comprised between the “LABEL_1” type labels [16, Sect. 7.7] #S_60DegSectorR200 and #E_60DegSectorR200. DIPOLE here, has an index $k = -0.03$, reference radius $R_0 \equiv R_0(E_k = 200 \text{ keV}) = 12.924888 \text{ cm}$ and $B_0 = B(R_0) = 0.5 \text{ T}$. Note that (i) this file can be run on its own: it has been designed to provide the transport MATRIX of that DIPOLE; (ii) for the purpose of some of the exercises, IL=2 under DIPOLE, optional, causes the printout of particle data in zgoubi.plt, at each integration step (this is at the expense of CPU time, and memory volume)

```
60DegSectorR200.inc
'OBJET'
64.62444403717985 ! 200keV proton.
5
0.01 0.001 0.01 0.001 0. 0.0001
12.924888074 0. 0. 0. 0. 1. ! 200keV. R=Brho/B=*/.5.
'DIPOLE' #S_60DegSectorR200 ! Analytical modeling of a dipole magnet.
2 ! IL=2, purpose: log stepwise particle data in zgoubi.plt. Avoid if unused: I/Os take CPU time.
60. 12.924888 ! Sector angle AT; reference radius R0.
30. 5. -0.03 0. 0. ! Reference azimuthal angle ACN; BM field at R0; indices, N, N', N''.
0. 0. ! EFB 1 is hard-edge,
4 .1455 2.2670 -.6395 1.1558 0. 0. 0. ! hard-edge only possible with sector magnet.
30. 0. 1.E6 -1.E6 1.E6 1.E6
0. 0. ! EFB 2.
4 .1455 2.2670 -.6395 1.1558 0. 0. 0.
-30. 0. 1.E6 -1.E6 1.E6 1.E6
0. 0. ! EFB 3 (unused).
0 0. 0. 0. 0. 0. 0. 0.
0. 0. 1.E6 -1.E6 1.E6 1.E6 0. 0.
4 10.
0.5 ! Integration step size. Small enough for orbits to close accurately.
2 0. 0. 0. 0. ! Magnet positioning RE, TE, RS, TS.
'FAISCEAU' #E_60DegSectorR200
'MATRIX'
1 0
'END'
```

Table 3.22 Simulation input data file: raytrace a few turns around the cyclotron, three particles with different momenta, and 0.1 mrad horizontal and vertical take-off angles. The INCLUDE segment is taken from Tab. 3.21

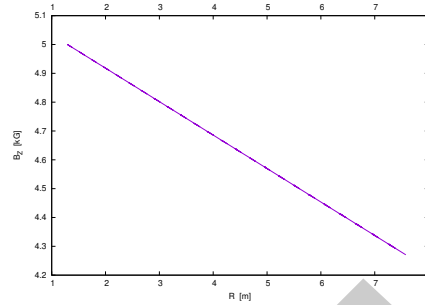
```
'MARKER' ProbProjTraj_S
'OBJET'
64.62444403717985 ! Reference Brho ("BORO" in the users' guide) -> 200keV proton.
2
3 1
12.924888 0.1 0. 0.1 0. 1. 'o' ! A particle with kin-E=0.2 MeV and 0.1 mrad take-off angles.
30.107898 0.1 0. 0.1 0. 2.2365445 'm' ! p[MeV/c]=433.306, Brho[kG.cm]=144.535, kin-E[MeV]=1.
75.754671 0.1 0. 0.1 0. 5.0063900 'o' ! p[MeV/c]=969.934, Brho[kG.cm]=323.535, kin-E[MeV]=5.
1 1 1
'INCLUDE'
1
6* 60DegSectorR200.inc[#S_60DegSectorR200:#E_60DegSectorR200] ! 6 sectors for an overall 360 deg.
'REBELOTE'
9 0.1 99 ! There will be a total of 9+1=10 turns.
'SYSTEM'
1
gnuplot < ./gnuplot_Zplt_traj.gnu ! Plot the projected Y(s) and Z(s) motions.
'MARKER' ProbProjTraj_E
'END'
```

A gnuplot script to obtain Fig. 3.41:

```
# gnuplot_Zplt_traj.gnu
set xtics nomirror; set x2tics; set ytics; set xlabel 's /C_E '; set ylabel 'Y [cm]'
set palette defined ( 1 "red", 2 "blue", 3 "black" ); unset colorbox
array R[3]; R[1]=0.12924888; R[2]=0.301078986; R[3]=0.75754671; pi = 4.*atan(1.); cm2m = 0.01
sector=3 # number (NOEL) of 1st DIPOLE in \zgoubi.res (col. 42 in zgoubi.plt)
# in zgoubi.plt, col. 19: particle number; col. 42: keyword number; col. 14: distance; col. 10: Y ; col. 12: YZ
plot for [sector=1:6] for [trj=1:3] 'zgoubi.plt' u ($19==trj && $42==sector1+2*(sector-1)? $14*cm2m/(2.*pi*R[$19]) :1/0) \
:($10*cm2m-R[trj]):($19) w p ps .2 lc palette notit ; pause 1

set ylabel 'Z [cm]'; plot for [sector=1:6] for [trj=1:3] 'zgoubi.plt' u ($19==trj && $42==sector1+2*(sector-1)? $14*cm2m \
/(2.*pi*R[$19]) :1/0):($12):($19) w p ps .2 lc palette notit ; pause 1
```

Fig. 3.40 In DIPOLE field model (Eq. 3.35), $\frac{\partial B}{\partial R}$ is constant: this graph shows the linear decrease of the field $B_Z(R)$ (Eq. 3.38), obtained from the raytracing of particles circulating in the median plane on orbits spanning a 0.2 to 5 MeV energy range



2608 with ΔR assumed small, $\partial B/\partial R = kB_E/R_E$ an energy independent quantity, and
 2609 the index E denoting a quantity taken at the reference energy. The latter property is
 2610 illustrated in Fig. 3.40, produced using the input data file of Tab. 3.23.

Table 3.23 Simulation input data file for a magnetic field scan. The INCLUDE segment is taken from Tab. 3.21

```
Field and derivative dB/dR, as a function of R
'MARKER' ProbProjTrajB_S
'OBJET'
64.62444403717985 ! Reference Brho ("BORO" in the users' guide) -> 200keV proton.
2
1 1 ! Just one ion.
12.924888 0.1 0. 0.1 0. 1. 'o' ! A particle with kin-E=0.2 MeV and 0.1 mrad take-off angles.
1
'INCLUDE'
1 ! IL=2 is necessary under DIPOLE, for step-by-step log of particle data in zgoubi.plt.
60DegSectorR200.inc[#_5_60DegSectorR200:#E_60DegSectorR200] ! One sector is enough.
'FIT'
1
2 30 0 [12,80] ! Vary particle's Y0 at OBJET, to have it match its D (=Brho/BORO).
1 1e-20
3.1 1 2 #End 0. 1. 0 ! Constrain Y_final=Y0.
'REBELOTE'
25 0.1 0 1 ! Scan parameter 35 (relative rigidity, D) in OBJET.
1
OBJET 35 1:5.00639 ! Scan relative rigidity D from 1 (200 keV) to 5.0063900 (5 MeV).
'SYSTEM'
1
gnuplot < ./gnuplot_Zplt_field.gnu ! Plot B(R), as read from zgoubi.plt.
'MARKER' ProbProjTrajB_E
'END'
```

A gnuplot script to obtain Fig. 3.40:

```
# gnuplot_Zplt_field.gnu
set xtics nomirror; set x2tics; set ytics; set xlabel 's /C_E'; set ylabel 'Y [cm]'
set palette defined ( 1 "red", 2 "blue", 3 "black" ); unset colorbox
array R[3]; R[1]=0.12924888; R[2]=0.301078986; R[3]=0.75754671; pi = 4.*atan(1.); cm2m = 0.01
sector1=3 # number (NOEL) of 1st DIPOLE in \zgoubi,res (col. 42 in zgoubi.plt)
# in zgoubi.plt, col. 19: particle number; col. 42: keyword number; col. 14: distance; col. 10: Y; col. 12: YZ
plot for [i=1:6] for [trj=1:3]
'zgoubi.plt' u ($19==trj && $42==sector1 +2*(i-1) ? $14*cm2m / (2.*pi*R[$19]) : 1/0) \
:($10*cm2m-R[trj]):($19) w p ps .2 lc palette notit ; pause 1

set ylabel 'Z [cm]' ;
plot for [i=1:6] for [trj=1:3]
'zgoubi.plt' u ($19==trj && $42==sector1 +2*(i-1) ? $14*cm2m \
/(2.*pi*R[$19]) : 1/0):($12):($19) w p ps .2 lc palette notit ; pause 1
```

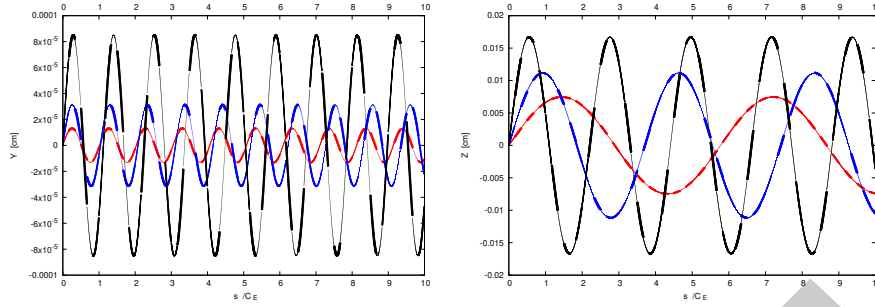


Fig. 3.41 Radial (left) and axial (right) paraxial motion around respectively the 200 keV (smallest amplitude), 1 MeV (intermediate) and 5 MeV (greatest amplitude) closed orbit (the latter is circular, in the median plane, with radius respectively $R_{200\text{ keV}} = 12.924888$ cm, $R_{1\text{ MeV}} = 30.107898$ cm and $R_{5\text{ MeV}} = 75.754671$ cm). The horizontal axis in this graph is s/C_E : path length over closed orbit circumference at energy E , the vertical axis is the motion excursion

2611 The resulting radial and axial motions over 10 turns are displayed in Fig. 3.41,
 2612 which also illustrates, for paraxial motion at some reference energy, the energy
 2613 dependence of the focusing strength (or wave number) and of the motion amplitude.

Table 3.24 Wave numbers, from numerical raytracing (columns denoted “ray-tr.”), from theory, and from discrete Fourier transform (‘DFT’ cols.) from a multi-turn tracking

E (MeV)	k_E	$\nu_R =$		$\nu_Z =$		
		ray-tr.	$\sqrt{1+k}$	ray-tr.	$\sqrt{-k}$	
0.2	-0.03	0.98520	0.9849	0.17320	0.1732	0.17321
1	-0.07279	0.96187	0.96292	0.26980	0.26979	0.26981
5	-0.20586	0.89083	0.89115	0.45326	0.45371	0.45371

An estimate of the wave numbers can be obtained as the inverse of the number of turns per oscillation, namely,

$$\nu_R = \frac{C_E}{\Delta s_M} \Big|_E \quad \text{and} \quad \nu_Z = \frac{C_E}{\Delta s_M} \Big|_E$$

2614 with Δs_M the measured distance between two consecutive maxima in the sinusoid
 2615 of concern in Fig. 3.41, C_E the closed orbit length for the energy of concern. Both
 2616 quantities are obtained from motion records in zgoubi.plt. This yields the values
 2617 of Tab. 3.24, where they are compared with the theoretical expectations, namely
 2618 (Eq. 3.18), $\nu_R = \sqrt{1+k}$ and $\nu_Z = \sqrt{-k}$.

2619 The maximum amplitude of the oscillation is obtained from zgoubi.plt records as
 2620 well, this yields the results of Tab. 3.25. For comparison, the theoretical values are
 2621 (Eqs. 3.16, 3.17 with respectively $x_0 = 0$, $x'_0 = T_0$ and $y_0 = 0$, $y'_0 = P_0$) $\hat{Y} = T_0 \frac{R_E}{\sqrt{1+k}}$
 2622 and $\hat{Z} = P_0 \frac{R_E}{\sqrt{-k}}$, wherein R_E denotes the closed orbit radius at energy E (for the
 2623 record: $R_E \equiv R_0$ at energy $E = 200$ keV, in the foregoing).

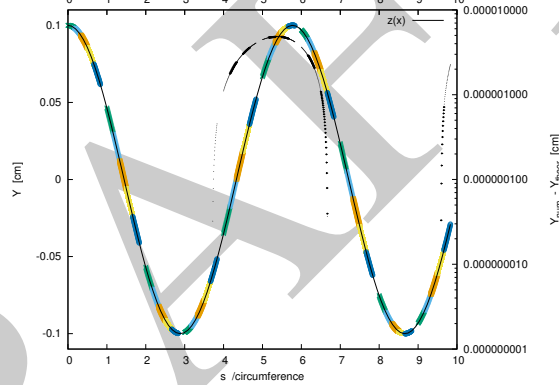
Table 3.25 Maximum amplitude of the oscillation, from raytracing (columns denoted “ray-tr.”) and from theory. R_E is the closed orbit radius for the energy of concern, $T_0 = P_0 = 0.1$ mrad is the trajectory angle at the origin, positions at the origin are zero

E (MeV)	k	\hat{Y}		\hat{Z}	
		ray-tr. $T_0 \frac{R_E}{\sqrt{1+k}}$ ($\times 10^{-5}$)	1.3125	ray-tr. $P_0 \frac{R_E}{\sqrt{-k}}$ ($\times 10^{-5}$)	7.4624
0.2	-0.03	1.3123	1.3125	7.4622	7.4624
1	-0.072787	3.1270	3.1267	1.1160	1.1160
5	-0.20586	8.5010	8.5008	1.6697	1.6697

2624 (c) Comparison with theory.

2625 Figure 3.42 shows the difference between numerical and theoretical vertical motion
 2626 excursion, using an *ad hoc* gnuplot script. An integration step size $\Delta s = 2$ cm is
 2627 used in the numerical integration.

Fig. 3.42 Vertical excursion of a 1 MeV trajectory over 20 turns (left vertical axis), and difference with theoretical expectation as per Eq. 3.17 (right vertical axis). The plot shows two sinusoidal curves: a segmented one, thicker, from numerical integration, and a thinner one, superimposed, from Eq. 3.17



2628 (d) A scan of energy dependence of wave numbers.

2629 A scan of the wave numbers over 200 keV–5 MeV energy range, computing tunes
 2630 with MATRIX, is performed using the input data file given in Tab. 3.26 (essentially
 2631 a copy of the input data file of Tab. 3.23, with an INCLUDE accounting for 6
 2632 DIPOLES [16, *lookup* INDEX]).

2633 OBJET[KOBJ=5] generates 13 particles with paraxial horizontal, vertical and
 2634 longitudinal sampling, proper to allow the computation of the first order transport
 2635 coefficients and wave numbers by MATRIX. REBELOTE repeats MATRIX computation
 2636 for a series of different particle rigidities. It is preceded by FIT which finds the
 2637 closed orbit. MATRIX includes a PRINT command, which causes the transport
 2638 coefficients (and various other outcomes of MATRIX computation) to be logged
 2639 in zgoubi.MATRIX.out. This allows producing the graphic in Fig. 3.43 - using the
 2640 gnuplot script given at the bottom of Tab. 3.26.

Table 3.26 Simulation input data file: for this wave number scan, the INCLUDE segment is taken from Tab. 3.21

```

Field and derivative dB/dR, as a function of R
'MARKER' ProbMATRIX_S
'OBJET'
64.62444403717985          ! Reference Brho ("BORO" in the users' guide) -> 200keV proton.
5                          ! Define 13 particles for MATRIX computation.
.001 .01 .001 .01 .001 .00001          ! Sampling of the initial coordinates.
12.924888 0. 0. 0. 1.          ! Reference: p[MeV/c]=193.739, Brho[kG.cm]=BORO, kin-E[MeV]=0.2.
'INCLUDE'
1          ! IL=2 is necessary under DIPOLE, for step-by-step log of particle data in zgoubi.plt.
6* 60DegSectorR200.inc[#S_60DegSectorR200:#E_60DegSectorR200]          ! Six 60 degree sectors.
'FIT'
1
2 30 0 [12,80]          ! Vary particle's Y0 at OBJET, to have it match its D (=Brho/BORO).
1 1e-10
3.1 1 2 #End 0. 1. 0          ! Constrain Y_final=Y0.
'MATRIX'
1 11 PRINT          ! PRINT: log computation outcome data to zgoubi.MATRIX.out, for further plotting.
'REBELOTE'
25 0.1 0 1          ! Scan parameter 35 (particle 1's D) in OBJT.
1
OBJET 35 1:5.00639
'SYSTEM'
1
gnuplot < ./gnuplot_MATRIX_Qxy.gnu
'MARKER' ProbMATRIX_E
'END'

```

A gnuplot script to obtain Fig. 3.43:

```

# gnuplot_MATRIX_Qxy.gnu
set xlab "kin. E [MeV]"; set ylab "{/Symbol n}_x, ({/Symbol n}_x^2+{/Symbol n}_y^2)^{1/2}"; set y2label "{/Symbol n}_y"
set key t l maxrow 1; set xtics; set ytics nomirror; set y2tics nomirror
BORO = 64.62444403717985; am = 938.27203e6; c = 2.99792458e8; BrhoRef = BORO *1e-3; eV2MeV = 1e-6
plot "zgoubi.MATRIX.out" u ((sqrt(($47*BrhoRef*c)**2 + am*am)-am)*eV2MeV):(556) w lp pt 5 lt 1 lw .5 lc rgb "red" \
tit "{/Symbol n}_x " , \
"zgoubi.MATRIX.out" u ((sqrt(($47*BrhoRef*c)**2 + am*am)-am)*eV2MeV):(557) axes xly2 w lp \
pt 6 lt 3 lw .5 lc rgb "blue" tit "{/Symbol n}_y " , \
"zgoubi.MATRIX.out" u ((sqrt(($47*BrhoRef*c)**2 + am*am)-am)*eV2MeV):(sqrt($56**2+$57**2)) \
w lp pt 7 lt 1 lw .5 lc rgb "black" t " ({/Symbol n}_x^2+{/Symbol n}_y^2)^{1/2}"; pause 1

```

Fig. 3.43 A scan of the energy dependence of the horizontal and vertical wave numbers. Markers are from raytracing, solid lines are from theory (Eq. 3.18). The figure also shows that the raytracing yields $\nu_R^2 + \nu_y^2 = 1$, $\forall E$, as expected

